

Removal Of Inorganic Contaminantsfrom Surface And Groundwater By Using NF/RO Filtration System

Hamad N. Altalyan^a, Brian Jones^b, John Bradd^b.

^a King Fahad Naval Academy, King Abdullaziz Naval Base, Al Jubail, Saudi Arabia.

^b School of Earth and Environmental Sciences, University of Wollongong, NSW 2522, Australia.

Corresponding Author:Hamad N. Altalyan

ABSTRACT

A comprehensive study was conducted to examine the removal of inorganic contaminants which exist in surface and groundwater in the Illawarra and Sydney regions. The ability of nanofiltration (NF) and reverse osmosis (RO) systems was investigated using two commercially available NF/RO membranes. Laboratory-scale tests used a cross-flow cell; tests were conducted with 10 ubiquitous solutions that represent the significant inorganic cations and anions commonly found in contaminated surface water.

This study concluded that the removal efficiency of RO was better than NF in rejecting the inorganic contaminants detected in surface water. This study revealed that the performance of the NF and RO membranes in rejecting divalent ions was higher than that for monovalent ion rejection and this can be attributed to multivalent ions with large hydrated radii (e.g. Mg²⁺ and SO₄²⁻) being retained more than monovalent ions with smaller hydrated radii (e.g. K⁺ and Na⁺). The removal efficiency of the NF membrane ranged from 85.9 to 98.3 % for cations, compared with anions, which showed a lower rejection ranging from 71.4 to 99 %. In contrast, the removal efficiency of the RO membrane ranged from 94.1 to 98.4 % for cations while anion rejection ranged from 89.5 to 99.7 %.

KEYWORDS:

Reverse osmosis (RO)

Nanofiltration (NF)

Botany Bay

Russell Vale

Date Of Submission:01-10-2018

Date Of Acceptance: 12-10-2018

I. INTRODUCTION

In recent years, the occurrence and fate of inorganic contaminants in the aquatic environment has been recognized as a significant issue of concern [1, 2]. Although there is full agreement between the scientific community and the water authorities to minimize inorganic contaminants, there is also an urgent need to make further efforts to protect water sources from these contaminants using optimized removal during water treatment processes. Recent trends towards reuse of reclaimed surface and groundwater for many purposes, in particular for agricultural and industrial sectors, encourages use of effective treatment to remove inorganic contaminants from contaminated water. During the last decades, numerous technologies have presented innovative solutions to the surface and groundwater contamination issue. For example, inorganic effluent can be removed by conventional treatment processes such as chemical precipitation, ion exchange and electrochemical removal [3]. However, it is well known that these

technologies are inadequate to remove and reduce all the inorganic contaminants to acceptable regulatory standards. Hence, there has been a growing interest during the last decade, for effective treatments such as membrane filtration (reverse osmosis [RO], nanofiltration [NF], ultrafiltration [UF] and microfiltration [MF]; [1]).

Nowadays, RO and NF membranes have become the leading technologies to treat numerous surface, well, brackish, urban and sea waters to produce fresh water [4-6]. NF/RO is able to remove several inorganic contaminants (such as arsenic, calcium, chloride, copper, fluoride, magnesium, manganese, nickel, nitrate, potassium, selenium, sodium, strontium, sulphate and zinc), which can be undesirable when above guideline standards for both health and aesthetic reasons [2, 7, 8].

Several studies have revealed that the separation of inorganic contaminants is affected by the compound's physicochemical properties and the membrane properties, as well as the solution chemistry [9, 10]. The separation of salts and inorganic contaminants is mostly attributed to size

exclusion as well as Donnan exclusion (charge repulsion mechanism; [11-14]). However, ionic permeation studies show that ionic size alone does not explain the rejection characteristics of ions during membrane filtration processes [15]. In the electrostatic repulsion mechanism, the rejection depends on relative charge interaction and not only on molecule size. Thus, electrostatic interactions between charged solutes and the charged membrane surface can also play a role in the rejection [2]. Moreover, it has been established that hydrophobic solutes can adsorb onto membrane surfaces and subsequently may diffuse through RO and particularly NF membranes, causing lower rejections than would be expected based solely on size exclusion mechanisms [16, 17]. On the other hand, ion transport is considerably affected by hydrated radii and hydration strength because size variations can determine which ions are capable of passing through the membrane pores by means of convection or diffusion. Ions with comparatively smaller ionic radii (i.e., Mg^{2+} and Ca^{2+}) have higher charge, higher hydration numbers, larger hydrated radii and hold hydration shells more strongly. In contrast, ions with larger ionic radii (i.e., K^+ and Na^+) have weaker hydration shells and smaller hydrated radii, and hence may be capable of separating from their hydration layer when passing through the membrane [18].

The aim of this study was to examine the removal of inorganic contaminants by using NF/RO filtration systems. Experiments were conducted using a laboratory-scale experiment with two commercially available NF/RO membranes. Ten inorganic compounds with molecular weights of less than 100 g/mol and a wide range of ionic and hydrated radii were selected as model inorganic contaminants due to their widespread occurrence in surface and groundwater. Removal efficiency by NF/RO filtration was linked to the physicochemical properties of these compounds to focus on the ability and effectiveness of this kind of treatment. Significant characterization work has been conducted to investigate the NF/RO membranes.

1.1 Study area

In this study contaminated groundwater samples have been collected from drillhole WGB32 at Botany Bay and a leachate pond at Russell Vale (Fig. 1) in the Sydney region.

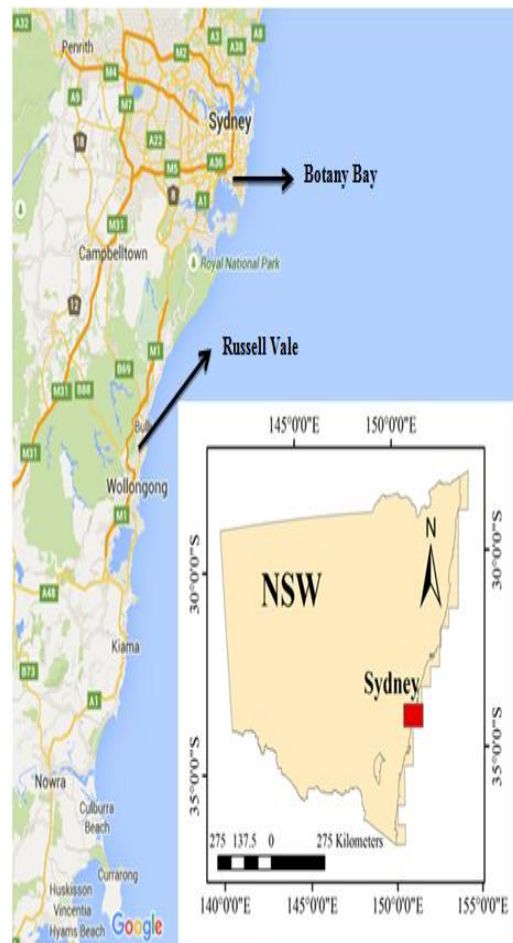


Fig. 1: Image illustrates samples sites in the Sydney regions.

II. MATERIALS AND METHODS

2.1 Laboratory-scale NF/RO filtration system

A laboratory-scale, cross-flow membrane filtration system with a stainless steel cross-flow cell was constructed for this study (Fig. 2). The cell had an effective membrane area of 40 cm^2 ($4\text{ cm} \times 10\text{ cm}$) and a channel height of 2 mm. The system was equipped with a Hydra-Cell pump (Wanner Engineering Inc., Minneapolis, MN). The temperature of the test solution was kept stable using a Neslab RTE 7 chiller/heater equipped with a stainless steel heat exchanger coil that was submerged directly into a stainless steel reservoir. The permeate flow was measured by a digital flow meter (Optiflow 1000, Agilent Technologies, Palo Alto, CA) connected to a personal computer, and the cross-flow rate was monitored using a rotameter.

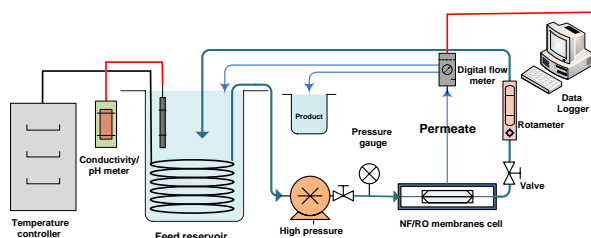


Fig. 2: Schematic diagram of the laboratory-scale pressure driven membrane filtration system

2.2. NF/RO membranes

A NF membrane (NF-90) and a RO membrane (ESPA2) were used in this project. NF-90 was obtained from Dow Film Tec (Minneapolis, MN, USA) whereas the ESPA2 was obtained from Nitto Denko (Oceanside, CA, USA). These membranes were received as flat sheet samples and stored dry. All membranes used in this study are made of a thin aromatic (or semiaromatic) polyamide active layer and thicker more porous supporting layer. Physicochemical characteristics of these membranes are illustrated in Table 1. Based on their estimated pore size, the NF-90 membrane could be classified as a tight nanofiltration membrane whereas ESPA2 can be assumed to have no obviously defined pore structure.

Table 1: Properties of the selected NF/RO membranes.

Membrane	Average pore Diameter ^a (nm)	Na ⁺ rejection ^b (%)	Molecular weight cut-off ^c (g/mol)	Contact angle ^d (°)	Surface roughness ^d (nm)
NF-90	0.68	85.0	~200	42.5	63.9
ESPA2	Not applicable	96.5	~100	60.6	30.0

^a[19].

^bFeed solution contains 20 mM NaCl and 1 mM CaCl₂ (pH 8).

^c Provided by the manufacturers.

^d[20].

2.3. NF/RO membrane characterisation

The surface streaming potential of the membrane was measured using a SurPASS Electrokinetic Analyzer (Anton Paar GmbH, Graz, Austria) in a 1 mM KCl background solution. To calculate the zeta potential from the measured streaming potential the Fairbrother–Mastin method was used, which was performed at 500 mbar and at room temperature ($25 \pm 1^\circ\text{C}$). The zeta potential of each membrane sample was measured four times, by repeatedly reversing the direction of electrolyte

flow at each pH value. Apparatus error counted for less than 0.5 mV of the measurement at any given pH value. Analytical grade potassium hydroxide and hydrochloric acid were used to regulate the pH via automatic titration.

According to Alturki et al. [20] the contact angle can be measured with a Rame-Hart Goniometer (Model 250, Rame-Hart, Netcong, NJ) by means of the standard sessile drop method. Milli-Q water is used as the reference solvent. The membranes are air dried before the measurement. No less than 5 droplets are applied onto duplicate membrane samples and contact angle is measured on both sides of the droplet.

The surface topography for NF/RO membranes was investigated by means of atomic force microscopy (AFM). On the other hand, the surface morphology and distribution of inorganic compounds deposited on the membrane surface were examined using field-emission scanning electron microscopy (SEM) on a JEOL JSM-7500FA - (BRUKER-QUANTAX 400), with additional semi-quantitative energy dispersive spectrometer (EDS) analyses

2.4. Model inorganic contaminants

Ten compounds were chosen for this study to represent two major inorganic groups of concern in surface and groundwater samples – namely cations (e.g. mercury, sodium and calcium) and anions (e.g. chloride, nitrate and sulphate). The selection of these model inorganic compounds was also based on their widespread occurrence in aquatic resources and their diverse physicochemical properties (e.g. molecular weight, ionic hydrated radii and hydrophobicity). The main physicochemical properties of these inorganic constituents are shown in Table 2. The selected inorganic contaminants include compounds with molecular weights in the range between 22.99 g/mol (paracetamol) and 96.06 g/mol. The retention of these compounds correlated with both charge and hydrated size. Therefore, multivalent ions with large hydrated radii (i.e. Ca²⁺ and SO₄²⁻) were retained more than monovalent ions with smaller hydrated radii (i.e. Cl⁻, K⁺ and Na⁺; [2]). Additionally, the quantity of charge on the surface of the membrane impacts the degree of electrostatic repulsion and removal of negatively charged solutes [21].

Table 2:Molecular weight, ionic and hydrated radii for relevant cations and anions.

Ion	Molecular weight (g/mol)	Ionic radius (nm)	Hydrated radius (nm)	Ref.
Na⁺	22.99	0.095	0.358	[22]
Ca²⁺	40.08	0.100	0.412	[23]
K⁺	39.10	0.133	0.331	[22]
Mg²⁺	24.31	0.065	0.428	[22]
Hg⁺	200.59	0.119	NA ^a	[24]
SO₄²⁻	96.06	0.215	0.300	[25]
PO₄³⁻	95.0	0.223	0.339	[25]
NO³⁻	62.00	0.264	0.335	[22]
Cr	35.45	0.181	0.332	[22]
Br⁻	79.90	0.195	0.330	[22]

^a NA: Not available.

2.5.Inorganic compounds analysis

All samples collected before and after filtration using both the NF/RO filtration system were analysed at ORICA Botany Environmental Laboratories. Cations, anions and mercury were analysed by using ICP-OES, IC, FIMS and GC-MS, ICP, respectively.

Cations were digested with aqua regia at 95 °C for 2 hours and then analysed with a Perkin Elmer Optima 7000DV ICP-OES (inductively coupled plasma optical emission spectrometry) based on the US EPA Method 200.7. According to this technique, samples are nebulised and the consequent aerosol is transferred to the plasma torch. Production of specific emission spectra for any element is obtained by radio-frequency inductively coupled plasma. The spectra are distributed by a grating spectrometer, and the intensities of the line spectra are checked at definite wavelengths by a photosensitive device. Photocurrents from the photosensitive device are processed and managed by a computer system. A background correction technique is essential to compensate for mutable background participation to the determination of the analysis. Background has to be measured adjacent to the analysed wavelength during analysis and several interferences must be taken into consideration (USEPA Method.200.7[26]).

Anions were analysed using Metrohm 881 Compact IC Pro Suppression Ion Chromatography based on "Standard methods for the examination of water and wastewater" (American Public Health Association, 2005, American Water Works Association, 2005 and Water Environment Federation, 2005, Method 4110.B). This method is appropriate, after a filtration process to eliminate solid particles using a 0.2µm pore diameter membrane filter. By this method the common anions such as bromide, chloride, fluoride, nitrate, nitrite, phosphate and sulfate can be determined. Basically, this method uses a prewashed syringe of 1 to 10 mL capacity equipped with a male luer suitable injecting sample or standard. Inject sufficient sample to flush the sample loop many times: for a 0.1 mL sample loop inject at least 1 mL. Shift the ion chromatograph from load to inject mode and record peak heights and retention times on a strip chart recorder. After the last peak (SO_4^{2-}) has performed and the conductivity signal has returned to the base line, another sample can be injected. Compute the concentration of each anion, in milligrams per litre, by referring to the appropriate calibration curve. Otherwise, when the response is shown to be linear, use the following equation:

$$C = H \times F \times D \quad (1)$$

Where C = mg anion/L, H = peak height or area, F = response factor = concentration of standard/height (or area) of standard, and D = dilution factor for those samples requiring dilution [27]

Mercury was digested with aqua regia at 95 °C for 2 hours, and then analysed using a Perkin Elmer FIMS 400 (Flow injection mercury system) according to Method 7470. Method 7470 is a cold-vapor atomic absorption process accepted for determining the concentration of mercury in mobility-procedure extracts, aqueous wastes and groundwaters. This vapor atomic absorption technique is based mainly on the absorption of radiation at 253.7nm by mercury vapour. The mercury is reduced to the elemental status and ventilated from solution in a sealed system. In the next step, the mercury vapor passes through a cell located in the light path of an atomic absorption spectrophotometer. Absorbance (peak height) is measured as a function of mercury concentration [28].

2.6. Analysis of basic water parameters

The temperature, turbidity, dissolved oxygen (DO), electrical conductivity (EC), total dissolved solids (TDS), salinity, (SG) and redox (water quality parameters) were measured using Water Quality Analyser-MODEL 516 during sampling (see Table 3 and Table 4). On the other

hand, the temperature, conductivity and pH were measured using an Orion 4-Star Plus pH/conductivity meter in all experiments. The measurements were applied at 0 time, one hour and at 8 hours for each experiment.

Table 3: Water quality parameters for samples which were collected from the leachate at pond-Russell Vale Golf Course ^a.

Season	Depth (m)	Turbidity (ntu)	Dissolved Oxygen (mg/l)	Electrical conductivity (μS/cm)	Total Dissolved Solids (g/l)	pH	Temperature (°C)	Salinity (ppt)	SG (t/m³)	Redox (mV)
Spring	0.33	99	3.43	3442	2.129	8.55	15.01	1.72	1.000	+389
Summer	0.42	66.5	10.8	2761	1.66	8.23	21.76	1.45	0.999	+51
Autumn	0.49	178	7.40	2475	1.67	8.27	20.90	1.46	0.999	+500
Winter	0.50	105.1	7.75	1971	1.104	7.99	14.61	0.87	1.000	+387

^a All data were obtained using Water Quality Analyser (MODEL 516).

Table 4: Water quality parameters for samples which were collected from WGB32 located near the tennis courts outside the fenceline at ORICA^ainBotany Bay.

Season	Depth (m)	Turbidity (ntu)	Dissolved Oxygen (mg/l)	Electrical conductivity (μS/cm)	Total Dissolved Solids (g/l)	pH	Temperature (°C)	Salinity (ppt)	SG (t/m³)	Redox (mV)
Spring	5.75	2.1	2.41	8000	5.84	10.5	19.35	4.97	1.002	+540
Summer	5.80	2.6	1.47	7250	5.79	10.55	21.4	4.91	1.001	- 44
Autumn	5.75	2.5	1.42	7667	5.34	11	21.86	4.89	1.002	- 43
Winter	5.38	1.8	0.80	8000	5.58	10.57	19.45	4.77	1.002	+533

^a All data were obtained using Water Quality Analyser (MODEL 516).

2.7. NF/RO filtration protocol

Prior to each pressure driven filtration experiment, the membrane was compacted using Milli-Q water (8 L) for approximately 1 hour until a stable baseline flux was obtained. The compacting pressures were 12 and 18 bars for the NF and RO membranes, respectively. The Milli-Q water used for membrane compaction was replaced with 8 L of a solution containing contaminated surface or groundwater after filtration using a Stericup DuraporeTM 0.45 μm Millipore. The cross-flow velocity flux was adjusted to 30.4 cm/s. The feed reservoir temperature was kept constant at 20 ± 0.1 °C throughout the experiment. Both permeate and concentrate were recirculated back to the feed reservoir (Fig. 2). Permeate and feed samples of 250 and 100 mL (two duplicates) were collected after 1 hour and at 8 hours of filtration to analyse cations and anions respectively. The feed reservoir temperature was kept constant at 4 ± 0.1 °C throughout the experiment using an exceptional chiller device to avoid evaporation of these compounds. All samples collected both feed and

permeate were sent immediately to ORICA Botany Environmental Laboratories for analysis. The rejection rate is defined by Equation:

$$R = \left(1 - \frac{C_p}{C_f} \right) \times 100\% \quad (2)$$

Where C_p and C_f are the permeate and the feed concentrations, respectively.

III. RESULTS AND DISCUSSION

3.1. SEM-EDS analysis

The clean and fouled membranes were visually characterised with scanning electron microscopy while the elemental analysis was determined using an integrated energy-dispersive spectrometer (EDS). To visualize the fouling effects, SEM images of the membrane surfaces were taken before and after fouling (Figs. 1 and 2) for the ESPA2 and NF-90 membranes, respectively. Due to the roughness of NF and RO membranes, after filtration the colloids are located principally in the valleys on the surface; i.e. "valley clogging" has taken place [29, 30]. However, the

colloids are distributed over the entire membrane surface and formed a dense and uniform cake layer on the membrane surface as a result of hydrophobic

interactions between the foulants and the membrane surfaces [31, 32].

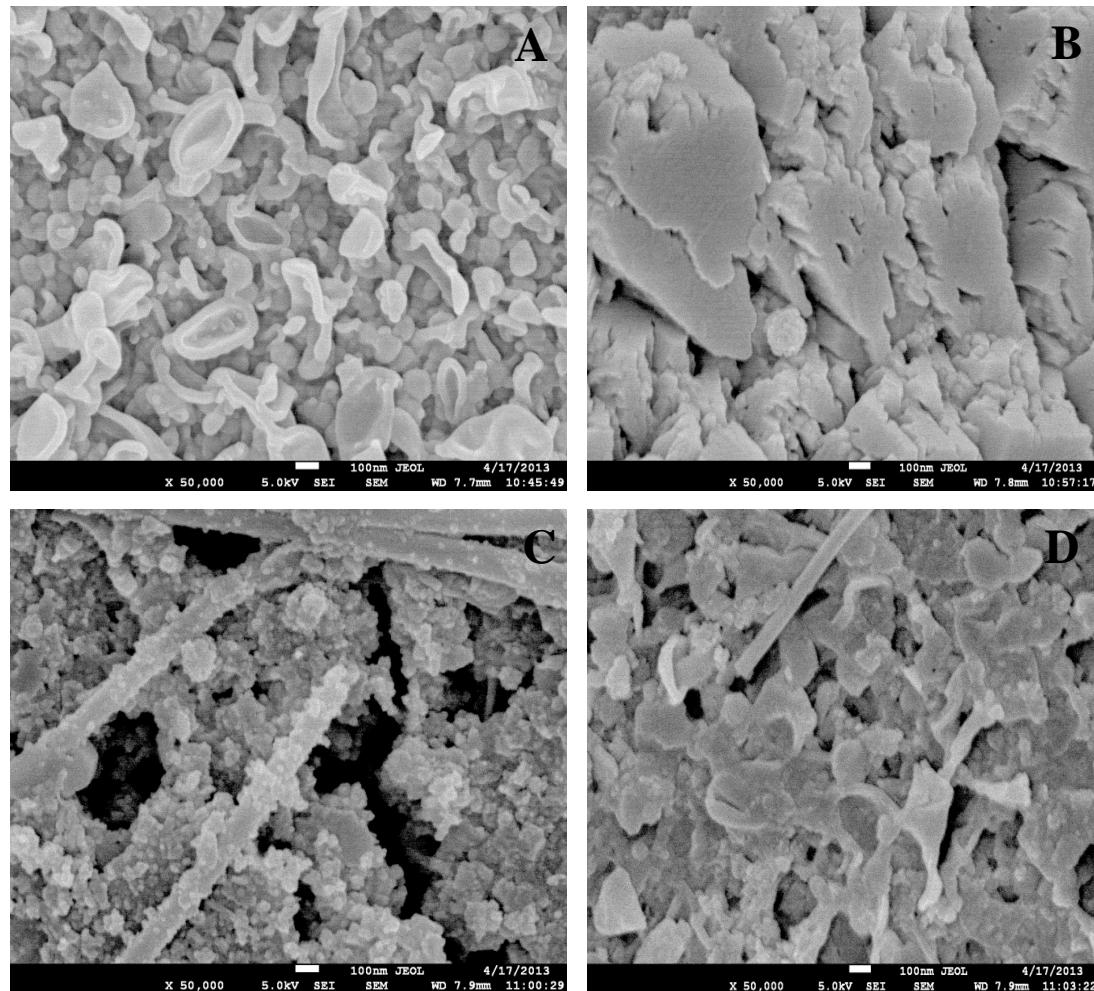


Fig. 1: SEM images of the (A) virgin ESPA2 membrane, (B) ESPA2 membrane surface fouled by leachate pond-autumn, (C) ESPA2 membrane surface fouled by WGB32-spring and (D) ESPA2 membrane surface fouled by WGB32-winter.

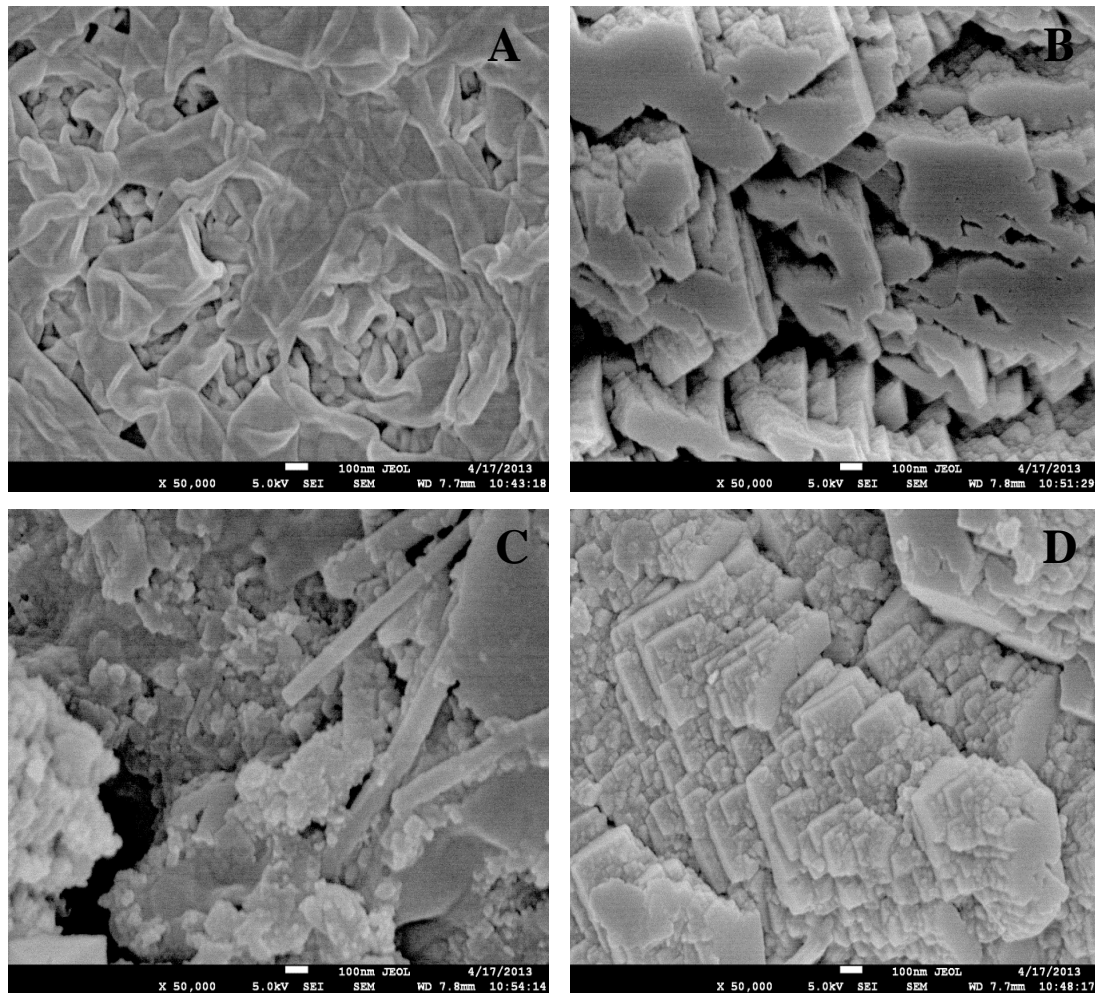


Fig. 2: SEM images of the (A) virgin NF-90 membrane, (B) NF-90 membrane surface fouled by leachate pond-autumn, (C) NF-90 membrane surface fouled by WGB32-spring and (D) NF-90 membrane surface fouled by leachate pond-summer.

Distribution of elements deposited in the fouling layer on the membrane surface was obtained from SEM with additional semi-quantitative EDS analysis. An example of SEM-EDS images obtained for the ESPA and NF-90 virgin and fouled membranes is shown in Figs. 3 and 4. In addition to the model foulants, carbon, oxygen and sulphur from the membrane polymeric composition were detected in all samples, including the virgin membrane. Noteworthy, platinum existed in all samples, including the virgin membrane as a result of membrane coating. A high level of calcium was found in the alginate fouling layer (Figs. 3B-2, 3B-3, 4B-2 and 4B-3) due to the ability of calcium to complex with carboxyl groups which are very common in organic foulants, in addition to the surface of the NF/RO membranes

[33]. This result is consistent with previous studies that calcium could make cross-links with alginate molecules and accumulate in the alginate fouling layer [34-36]. Specifically, a sulphur peak was observed with contaminated samples which were collected from WGB32 at Botany Bay indicating the participation of sulphate scale in fouling (see Figs. 4B-2 and 4B-3). Small silicon and aluminium peaks were noticed with membrane surfaces fouled by WGB32-Spring (Fig. 4B-3) indicating their high scaling tendency even when present in a small amount. Additionally, a small level of sodium and chlorine was found in the alginate fouling layer (Figs. 4B-2 and 4B-3). It can be explained by the deposition of foulants (Si, Al, Na and Cl) on the membranes caused by the increase in membrane selectivity due to biofouling [37].

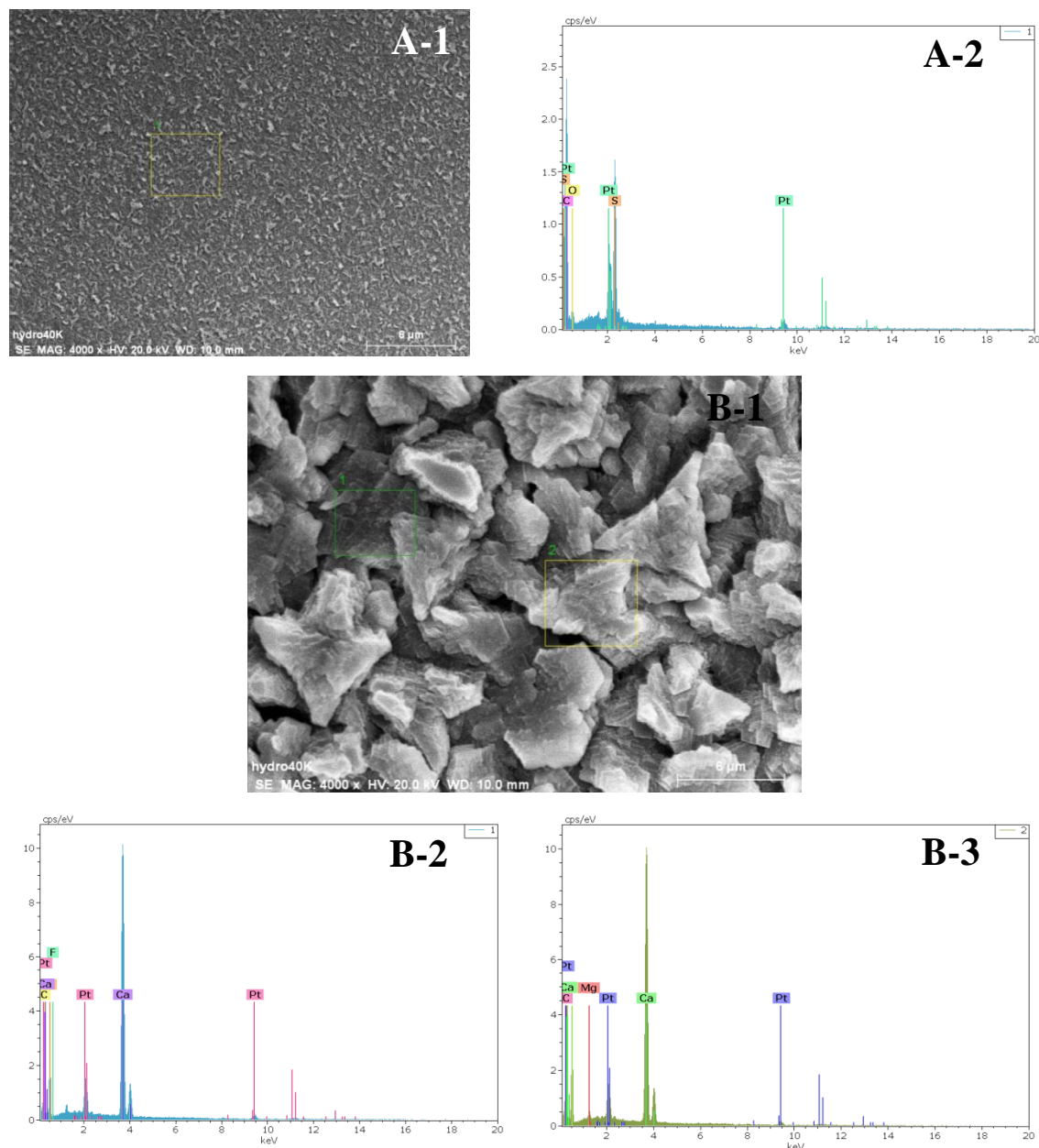


Fig. 3: EDS data of the virgin ESPA2 membrane (A-1and A-2) and ESPA2 membranefouled by leachate pond from Russell Vale - autumn (B-1, B-2 and B-3).

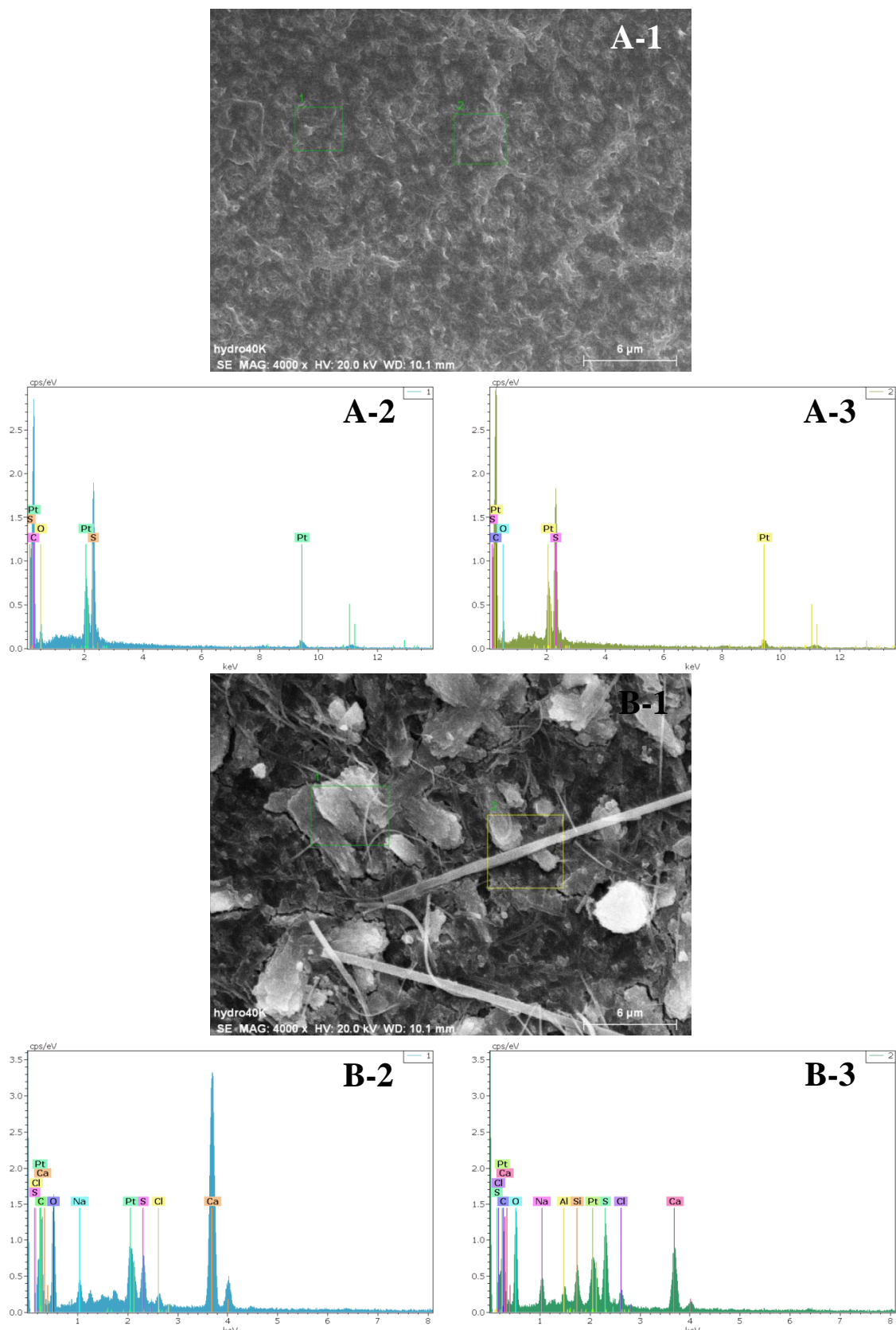


Fig. 4: EDS data of virgin NF-90 membrane (A-1, A-2 and A-3) and NF-90 membrane fouled by WGB32 at Botany Bay - spring (B-1, B-2 and B-3).

3.2 Removal of inorganic contaminants by the NF/RO system

To examine the ability of the NF/RO membranes to remove inorganic contaminants from contaminated surface and groundwater, many experiments were conducted at different seasons for samples collected from a leachate pond at Russell Vale Golf Course and WGB32 at Botany Bay.

3.2.1. Leachate pond at Russell Vale Golf Course

Contaminated surface water is represented by samples collected from a leachate pond at Russell Vale Golf Course during 2012 for four seasons. The removal efficiency for both NF-90 and ESPA2 membranes are reported in Fig. 5. The findings in Fig. 5 show that the performance of the NF-90 and ESPA2 membranes after 8 hours was better than after one hour. Further, it was observed that the ESPA2 membrane has a higher capability than the NF-90 membrane for rejecting cations and anions. Moreover, it was notable that the performance of the NF-90 and ESPA2 membranes in rejecting divalent ions was higher than that of its monovalent ion rejection and this is consistent with the findings from previous studies [8, 36, 38]. This phenomenon can be explained since multivalent ions with large hydrated radii (e.g. Mg^{2+} , Ca^{2+} and SO_4^{2-}) were retained more than monovalent ions with smaller hydrated radii (e.g. K^+ and Na^+ ; [2]). The removal efficiency of the NF-90 membrane ranged between 85.9 and 98.3 % for cations, compared with anions, which showed a slightly lower rejection ranging from 71.4 to 99.2 %. In contrast, the removal efficiency of the ESPA2 membrane ranged between 94.1 and 98.4 % for cations while anion rejection ranged between 89.5 and 99.7 %. It is noteworthy that the highest rejection achieved by both NF-90 and ESPA2 was for sulphate that reached 99.7% while the lowest rejection achieved by both NF-90 and ESPA2 was for bromide which amounted to 71.4 %. Also, as seen in Fig. 5 the performance of the NF-90 and ESPA2 membranes in rejecting the model foulants was high in all seasons except for the summer season in particular when the NF-90 was fouled by algal suspensions. This can be explained since the higher temperature during summer participates significantly in the growth of algae blooms [39]. Algae can release extracellular organic matter (EOM). This extracellular, mucilaginous slime material can raise resistance to filtration [40]. It has been observed that characteristics of EOM could significantly influence the specific cake resistance developed in membrane filtration [39].

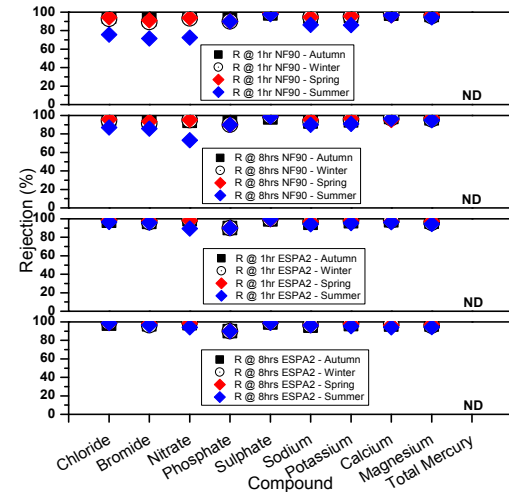


Fig. 5: Overall removal efficiency of the selected inorganic compounds which were detected in contaminated surface water at Russell Vale. NF/RO membrane filtration experiment was conducted at an initial permeate flux of $41 \text{ L/m}^2\text{h}$ at a temperature of 20°C and a cross-flow velocity of 30.4 cm/s . Samples were collected after 1 and 8 hours of filtration.

3.2.2. WGB32 at Botany Bay

Contaminated groundwater is represented by samples collected over four seasons from Orica (Botany Bay) in the Sydney area during 2012. An overall comparison of NF-90 and ESPA2 membrane performances in terms of removal efficiency is presented in Fig. 6 which shows that the performance of both membranes after 8 hours was better than after one hour. Moreover, it was noteworthy that the performance of the NF-90 and ESPA2 membranes in rejecting multivalent ions was higher than that of its monovalent ion rejection in particular for sulphate. This is consistent with both the results reported above and previous studies (e.g.[8]).

The removal efficiency of the NF-90 membrane ranged between 60 and 100 % for cations while anion rejection ranged between 64.8 and 99.5 %. On the other hand, the removal efficiency of the ESPA2 membrane ranged between 76 and 100 % for cations while anion rejection ranged from 76 to 99.7 %. It is remarkable that the highest rejection achieved by both NF-90 and ESPA2 was for total mercury and this compound was almost completely rejected, while the lowest rejection achieved by both NF-90 and ESPA2 was for calcium which amounted to 60%. Complete rejection of total mercury could be attributed to sieving (or size exclusion) as the molecular weight of mercury is 200.59 g/mol which is higher than the molecular weight cut-off (MWCO) of NF-90 and ESPA ($\sim 200 \text{ Da}$ and $\sim 100 \text{ Da}$). In other words, the sieving of large molecules occurs through the small membrane pores and this phenomenon is called the

stearic hindrance effect that operates principally for neutral solutes [41].

Furthermore, as shown in Fig. 6 the performance of the NF-90 and ESPA2 membranes in rejecting the model foulants was high in all seasons, except winter and spring in the case of NF-90 that was somewhat low. This result is consistent with the findings concluded in previous studies [42]. Reznik et al. [42] concluded that both loose (NF-270) and tight (NF-90) NF membranes, exhibited a high dependency on the water matrix and season for rejection of carbamazepine, where the rejection of this component was higher in summer ($84\pm5\%$ average and up to 92%) than in winter ($54\pm10\%$ average and down to 50%). Changes in the effluent organic matter seasonally produced during the biological stage could explain this phenomenon.

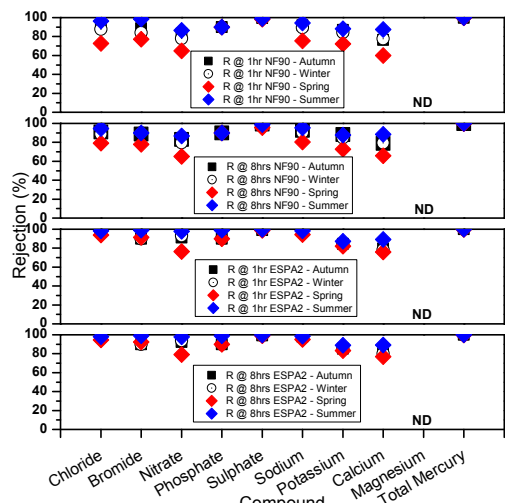


Fig. 6: Overall removal efficiency of the selected inorganic compounds which were detected in contaminated groundwater at Orica (Botany Bay). NF/RO membrane filtration experiment was conducted at an initial permeate flux of $41 \text{ L m}^{-2} \text{ h}^{-1}$ at a temperature of 20°C and a cross-flow velocity of 30.4 cm s^{-1} . Samples were collected after 1 and 8 hours of filtration.

3.3 Performance of the NF/RO membranes

To investigate the performance of NF/RO membranes, it is essential to study the membrane permeate flux as a function of filtration time for samples that were collected in different seasons and from different sites (leachate pond at Russell Vale and WGB32 at Botany Bay).

Table 5: Comparison between permeate flux decline (%) of the NF-90 and ESPA2 membranes for samples collected from the leachate pond at Russell Vale after 8 hours of filtration.

Season	Permeate Flux Decline of NF-90 (%) ^a	Permeate Flux Decline of ESPA2 (%) ^b
Autumn	45	69.7
Winter	47	19
Spring	27.3	14.4
Summer	85	83.4

^{a/b} Data calculated using following Equation: $\text{FluxDecline (\%)} = \left(1 - \frac{J}{J_0}\right) \times 100$

3.3.1. Leachate pond at Russell Vale Golf Course

Figures 7A and 7B show the evolution of the membrane permeate flux as a function of filtration time. Substantial permeate flux decline was observed with both the NF-90 and ESPA2 membranes in particular for samples that were collected in autumn and summer seasons from the leachate pond due to fouling of the membranes (Table 5). Fouling due to living cells, such as algae, is quite complex since these cells change their sizes, morphology, and have extracellular organic matter (EOM) attached to their cells. High temperatures and light intensity as well as nutrient availability in these two seasons inhibit the growth and photosynthesis process and result in high release of EOM. Consequently, the existence of EOM in the reservoir frequently clogs the pores of the membranes, leading to permeate flux decline [39]. Furthermore, as seen in Fig. 7 the permeate flux for the ESPA2 membrane (Fig. 7B) was better than the permeate flux for the NF-90 membrane (Fig. 7A) specifically in winter and spring seasons. There is a correlation between fouling tendency and the membrane surface roughness, and this strongly agrees with previous studies (e.g. [29, 32]). NF-90 has a significant surface roughness (63.9 nm) whereas ESPA2 has a rather smooth membrane surface with a corresponding surface roughness of 30.0 nm (Table 1). Indeed, with the exception of the autumn and summer seasons, where there was a significant decline of flux caused by fouling, the ESPA2 membranes (Fig. 7B) did not show any measurable flux decline over approximately 8 hours of filtration time in other seasons (winter and spring). In contrast, there was permeate flux decline for the NF-90 membrane in autumn and summer seasons and slight flux decline for winter and spring seasons (Fig. 7A). Also physicochemical properties of membranes, in particular pore size, could play a significant role in the extent of organic fouling. Permeate flux decline because of membrane fouling could be more severe with membranes having a larger pore size (NF-90) compared to ESPA2 (which is classified as nonporous). This conclusion is consistent with previous literature [43] which revealed that permeate flux decline is governed by the pore size of membrane.

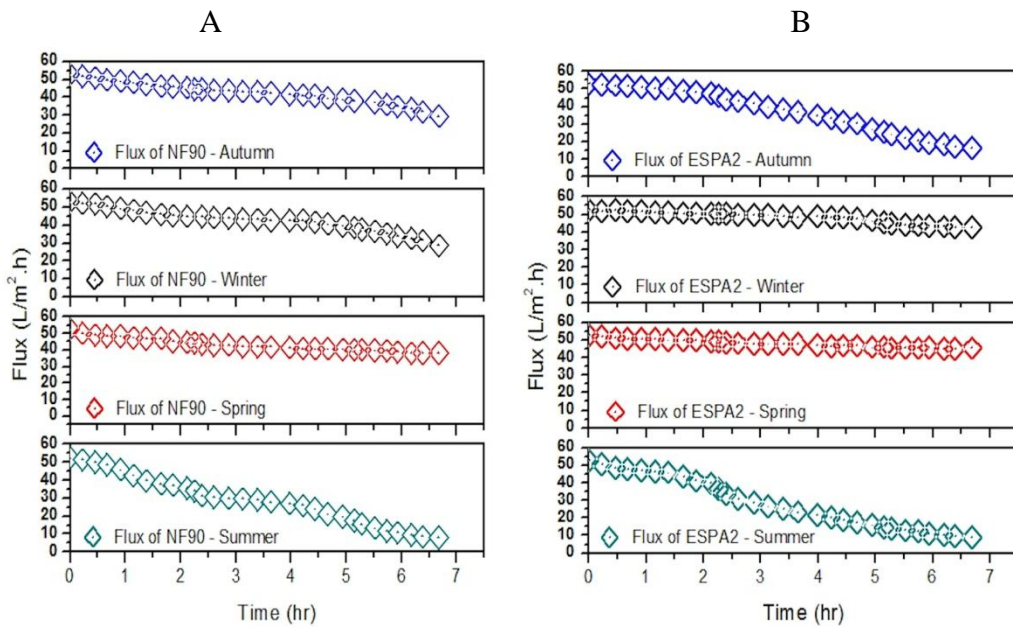


Fig. 7: Permeate flux of (A) NF-90 and (B) ESPA2 membranes as a function of filtration time. Experiments were conducted at an initial permeate flux of 41 L/m²h, temperature of 20 °C and cross-flow velocity of 30.4 cm/s. Permeate were collected after 8 hours of filtration. Data for samples collected from the leachate pond at Russell Vale.

3.3.2. WGB32 at Botany Bay

Figure 8 displays the evolution of the membrane permeate flux as a function of filtration time for WGB32. Significant permeate flux decline could be observed with the NF-90 membrane (Table 6 and Fig. 8A). A small, but however discernible, flux decline could also be observed with the ESPA2 membrane (Table 6 and Fig. 8B).

Obviously there is a correlation between fouling propensity and the membrane surface

roughness (Table 1) and this completely agrees with previous studies (e.g. [29, 32]). In fact, the ESPA2 membrane did not show any measurable flux decline over approximately 8 hours of filtration time. In contrast, there was slight permeate flux decline when using the NF-90 membrane in all seasons and this is consistent with several previous studies (e.g. [20]).

Table 6: Comparison between permeate flux decline (%) of the NF-90 and ESPA2 membranes for samples collected from WGB32 at Botany Bay after 8 hours of filtration.

Season	Permeate Flux Decline of NF-90 (%)	Permeate Flux Decline of ESPA2 (%)
Autumn	11.5	4.7
Winter	12.7	4
Spring	16	8.7
Summer	20	8.8

^{a/b} Data calculated using following Equation: $FluxDecline (\%) = \left(1 - \frac{J}{J_0}\right) \times 100$

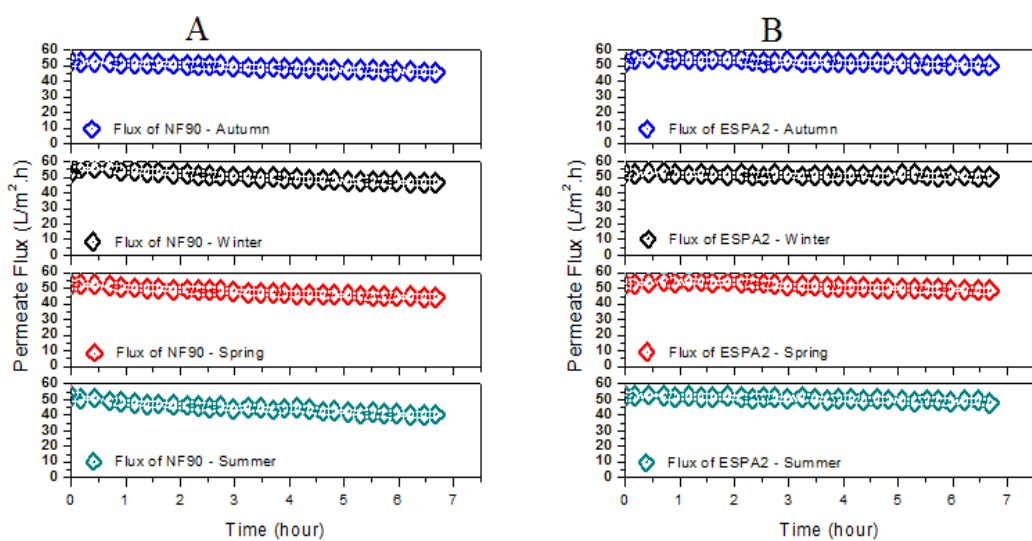


Figure 8: Permeate flux of (A) NF-90 and (B) ESPA2 membranes as a function of filtration time. Experiments were conducted at an initial permeate flux of 41 L/m²h, temperature of 20 °C and cross-flow velocity of 30.4 cm/s. Permeate were collected after 8 hours of filtration. Data for samples were collected from WGB32 at Botany Bay.

IV. CONCLUSIONS

Results reported in this study indicate that NF/RO membrane filtration can achieve enhanced removal efficiency for a wide range of inorganic contaminants detected in surface and groundwater collected from the leachate pond and WGB32, respectively. The findings of this study exhibited that the performance of the NF-90 and ESPA2 membranes after 8 hours was better than after one hour for the removal of model foulants at two sites (leachate pond and WGB32). Since the NF-90 has a significant surface roughness, the flux through this membrane declined significantly in autumn and summer and declined slightly for winter and spring for samples collected from the leachate pond. However the flux declined slightly in all seasons in case of samples collected from WGB32. In contrast, the ESPA2 has a somewhat smoother membrane surface and therefore it did not show any measurable flux decline over approximately 8 hours of filtration time for samples collected from WGB32. Nevertheless there was a significant decline in flux in autumn and summer for samples collected from the leachate pond. The considerable permeate flux decline both membranes with samples collected from the leachate pond in summer was due to the fouling. High temperatures and light intensity as well as nutrient availability in this season favoured the growth and photosynthesis process and result in large release of extracellular organic matter (EOM) from algae (e.g. *Microcystis aeruginosa*). Accordingly, the presence of EOM in the feed reservoir clogged the membranes leading to

permeate flux decline. The performance of the NF-90 membrane in rejecting the model foulants was high in all seasons except winter and spring in the case of samples collected from WGB32 and could be explained by differences in the effluent organic matter seasonally produced during the biological stage.

ACKNOWLEDGEMENTS

This study was supported by the Wollongong City Council and Orica. The Ministry of Defence in Saudi Arabia and the Royal Saudi Naval Forces is acknowledged for providing a PhD scholarship to Hamad Altalyan. I extend special thanks to all staff and students at the school of earth and environmental sciences for all the support and exchange of knowledge in a very friendly environment. I am greatly indebted to Mr Tony Romeo in the Electron Microscopy Centre, University of Wollongong, for his assistance and support with scanning electron microscope images. I would also like to thank our collaborators, James Stening, Sylvia Huo and Ivan Ward from Orica.

REFERENCES

- [1]. Ortega, L.M., et al., Removal of metal ions from an acidic leachate solution by nanofiltration membranes. Desalination, 2008. 227(1–3): p. 204-216.

- [2]. Richards, L.A., B.S. Richards, and A.I. Schäfer, Renewable energy powered membrane technology: salt and inorganic contaminant removal by nanofiltration/reverse osmosis. *Journal of Membrane Science*, 2011. 369(1-2): p. 188-195.
- [3]. Barakat, M.A., New trends in removing heavy metals from industrial wastewater. *Arabian Journal of Chemistry*, 2010. In Press, Corrected Proof.
- [4]. Nicolaisen, B., Developments in membrane technology for water treatment. *Desalination*, 2003. 153: p. 355-360.
- [5]. Bottino, A., et al., Membrane technologies for water treatment and agroindustrial sectors. *ComptesRendusChimie*, 2009. 12(8): p. 882-888.
- [6]. Norton-Brandão, D., S.M. Scherrenberg, and J.B. van Lier, Reclamation of used urban waters for irrigation purposes – a review of treatment technologies. *Journal of Environmental Management*, 2013. 122: p. 85–98.
- [7]. Sungyun, L., et al., Characterization of marine organic matters and heavy metals with respect to desalination with RO and NF membranes. *Desalination*, 2008. 221: p. 244–252.
- [8]. Alzahrani, S., et al., Comparative study of NF and RO membranes in the treatment of produced water -Part I: assessing water quality. *Desalination*, 2013. 315: p. 18–26.
- [9]. Nghiem, L.D. and P.J. Coleman, NF/RO filtration of the hydrophobic ionogenic compound triclosan: transport mechanisms and the influence of membrane fouling. *Separation and Purification Technology*, 2008. 62(3): p. 709-716.
- [10]. Watson, K., M.J. Farré, and N. Knight, Strategies for the removal of halides from drinking water sources, and their applicability in disinfection by-product minimisation: a critical review. *Journal of Environmental Management*, 2012. 110(0): p. 276-298.
- [11]. Yaroshchuk, A.E., Non-steric mechanisms of nanofiltration: superposition of Donnan and dielectric exclusion. *Separation and Purification Technology*, 2001. 22–23 p. 143–158.
- [12]. Teixeira, M.R., M.J. Rosa, and M. Nyström, The role of membrane charge on nanofiltration performance. *Journal of Membrane Science*, 2005. 265(1-2): p. 160-166.
- [13]. Verliefde, A.R.D., et al., The role of electrostatic interactions on the rejection of organic solutes in aqueous solutions with nanofiltration. *Journal of Membrane Science*, 2008. 322(1): p. 52-66.
- [14]. Bolong, N., et al., A review of the effects of emerging contaminants in wastewater and options for their removal. *Desalination*, 2009. 239(1-3): p. 229-246.
- [15]. Tansel, B., et al., Effect of transmembrane pressure on overall membrane resistance during cross-flow filtration of solutions with high-ionic content. *Journal of Membrane Science*, 2009. 328: p. 205–210.
- [16]. Nghiem, L.D. and A.I. Schäfer, Adsorption and transport of trace contaminant estrone in NF/RO membranes. *Environmental Engineering Science*, 2002. 19: p. 441-451.
- [17]. Braeken, L., et al., Influence of hydrophobicity on retention in nanofiltration of aqueous solutions containing organic compounds. *Journal of Membrane Science*, 2005. 252(1-2): p. 195-203.
- [18]. Tansel, B., et al., Significance of hydrated radius and hydration shells on ionic permeability during nanofiltration in dead end and cross flow modes. *Separation and Purification Technology*, 2006. 51: p. 40–47.
- [19]. Nghiem, L.D., A.I. Schäfer, and M. Elimelech, Removal of natural hormones by nanofiltration membranes: measurement, modeling, and mechanisms,. *Environ. Sci. Technol.*, 2004. 38 p. 1888–1896.
- [20]. Alturki, A.A., et al., Combining MBR and NF/RO membrane filtration for the removal of trace organics in indirect potable water reuse applications. *Journal of Membrane Science*, 2010. 365(1-2): p. 206-215.
- [21]. Xu, P., et al., Rejection of emerging organic micropollutants in nanofiltration-reverse osmosis membrane applications. *Water Environment Research*, 2005. 77: p. 40-48.
- [22]. Nightingale.E.R, Phenomenological theory of ion solvation. Effective radii of hydrated ions,. *Journal of physical chemistry*, 1959. 63: p. 1381–1387.
- [23]. Volkov, A.G., S. Paula, and D.W. Deamer, Two mechanisms of permeation of small neutral molecules and hydrated ions across phospholipid bilayers. *Bioelectrochemistry and Bioenergetics*, 1997. 42(2): p. 153-160.
- [24]. Haynes, W.M., T.J. Bruno, and D.R. Lide, *CRC Handbook of Chemistry and Physics*. 2013.
- [25]. Kiriukhin, M.Y. and K.D. Collins, Dynamic hydration numbers for biologically important ions. *Biophysical Chemistry*, 2002. 99(2): p. 155-168.

- [26]. Method.200.7, Determination of metals and trace elements in water and wastes by inductively coupled plasma atomic emission spectrometry (ICP-AES). 1994, United States Environmental Protection Agency: Ohio.
- [27]. Eaton, A.D., Standard Methods for the Examination of Water and Wastewater. 21st Ed ed. 2005, Washington: American Public Health Association; Water Environment Federation; American Water Works Association.
- [28]. Metod.7470A, Mercury in liquid waste (manual cold-vapor technique). 1994, USEPA.
- [29]. Vrijenhoek, E.M., S. Hong, and M. Elimelech, Influence of membrane surface properties on initial rate of colloidal fouling of reverse osmosis and nanofiltration membranes. *Journal of Membrane Science*, 2001. 188(1): p. 115-128.
- [30]. Hoek, M.V., S. Bhattacharjee, and M. Elimelech, Effect of membrane surface roughness on colloid-membrane DLVO interactions. *American Chemical Society*, 2003. 19(11): p. 4836-4847.
- [31]. Brant, J.A. and A.E. Childress, Membrane-colloid interactions: comparison of extended DLVO predictions with AFM force measurements *Environmental Engineering Science*, 2002. 19: p. 413-427.
- [32]. Boussu, K., et al., Influence of membrane and colloid characteristics on fouling of nanofiltration membranes. *Journal of Membrane Science*, 2007. 289(1-2): p. 220-230.
- [33]. Mo, Y., et al., A new perspective on the effect of complexation between calcium and alginate on fouling during nanofiltration. *Separation and Purification Technology*, 2011. 82: p. 121-127.
- [34]. Lee, S., W.S. Ang, and M. Elimelech, Fouling of reverse osmosis membranes by hydrophilic organic matter: implications for water reuse. 2006. 187: p. 313-321.
- [35]. Li, Q., Z. Xu, and I. Pinna, Fouling of reverse osmosis membranes by biopolymers in wastewater secondary effluent: role of membrane surface properties and initial permeate flux. *Journal of Membrane Science*, 2007. 229: p. 173-181.
- [36]. Antony, A., et al., Comparison of reverse osmosis membrane fouling profiles from Australian water recycling plants. *Journal of Membrane Science* 2012. 407-408: p. 8-16.
- [37]. Melián-Martel, N., et al., Structural and chemical characterization of long-term reverse osmosis membrane fouling in a full scale desalination plant. *Desalination*, 2012. 305(0): p. 44-53.
- [38]. Liikanen, R., I. Miettinen, and R. Laukkonen, Selection of NF membrane to improve quality of chemically treated surface water. *Water Research*, 2003. 37: p. 864-872.
- [39]. Babel, S., S. Takizawa, and H. Ozaki, Factors affecting seasonal variation of membrane filtration resistance caused by Chlorella algae. *Water Research*, 2002. 36: p. 1193-1202.
- [40]. Kwon, B., N. Park, and J. Cho, Effect of algae on fouling and efficiency of UF membranes. *Desalination*, 2005. 179: p. 203-214.
- [41]. Minhas, F.T., et al., Solvent resistant thin film composite nanofiltration membrane: characterization and permeation study. *Applied Surface Science*, 2013. 282(0): p. 887-897.
- [42]. Reznik, S.G., et al., Influence of seasonal and operating conditions on the rejection of pharmaceutical active compounds by RO and NF membranes. *Desalination*, 2011. 277: p. 250-256.
- [43]. Nghiem, L.D. and S. Hawkes, Effects of membrane fouling on the nanofiltration of trace organic contaminants. *Desalination*, 2009. 236(1-3): p. 273-281.